

## INTEGRATIVE QSAR ANALYSIS OF OXADIAZOLE DERIVATIVES: RESOLVING MOLECULAR DETERMINANTS FOR ANTI-TUBERCULAR ACTIVITY AND RATIONAL DRUG DESIGN

NEHA H. SUVARNA<sup>1</sup>, JESSY ELIZABETH MATHEW<sup>1</sup>, VIKSHITH RAJ<sup>1</sup>, SHIHABUDHEEN HAREES<sup>1</sup>, LALIT KUMAR<sup>2</sup>, RUCHI VERMA<sup>1\*</sup>

<sup>1</sup>Department of Pharmaceutical Chemistry, Manipal College of Pharmaceutical Sciences, Manipal Academy of Higher Education, Manipal-576104, Karnataka, India. <sup>2</sup>Department of Pharmaceutics, National Institute of Pharmaceutical Education and Research, Hajipur, Bihar, India  
\*Corresponding author: Ruchi Verma; \*Email: ruchi.verma@manipal.edu

Received: 16 May 2024, Revised and Accepted: 15 Jul 2024

### ABSTRACT

**Objective:** In this study, we conducted a comprehensive Quantitative Structure-Activity Relationship (QSAR) analysis of an oxadiazole derivative exhibiting potent anti-tubercular activity by inhibiting synthesis.

**Methods:** Our investigation employed both 3D atom-based and field-based Comparative Molecular Field Analysis/Comparative Molecular Similarity Indices Analysis (CoMFA/CoMSIA) techniques, along with auto QSAR analysis using a 2D canvas. The CoMFA and CoMSIA methodologies allowed for the exploration of molecular interactions and structural features contributing to the molecule's inhibitory potency. Utilizing these 3D approaches, we delineated the steric, electrostatic, hydrophobic, and hydrogen bond acceptor/donor fields influencing the molecular activity. Furthermore, the auto QSAR analysis provided valuable insights into the 2D structural descriptors governing the anti-TB efficacy of the oxadiazole compound.

**Results:** Our findings not only elucidate the molecular determinants essential for inhibitory activity but also provide a robust predictive model for assessing the anti-TB activity of structurally related compounds. Both 3D QSAR and 2D QSAR models were designed and generated. These models were found to be useful in predicting the anti-TB activity of oxadiazole derivatives. The best model for accurately predicting activity was found to have a Q<sup>2</sup> value of 0.9558 and an R<sup>2</sup> value of 0.979.

**Conclusion:** This integrative QSAR study contributes to the rational design and optimization of novel oxadiazole-based therapeutics against tuberculosis, addressing the urgent need for effective treatment strategies against this global health threat.

**Keywords:** QSAR, QSARCOMFA, COMSIA

© 2024 The Authors. Published by Innovare Academic Sciences Pvt Ltd. This is an open access article under the CC BY license (<https://creativecommons.org/licenses/by/4.0/>) DOI: <https://dx.doi.org/10.22159/ijap.2024v16i5.51468> Journal homepage: <https://innovareacademics.in/journals/index.php/ijap>

### INTRODUCTION

In 2022, the global Tuberculosis (TB) situation recorded 1.3 million deaths, with 167,000 individuals having both TB and HIV. TB is ranked as the second leading infectious cause of death globally following COVID-19, including its impact on HIV and AIDS. Around 10.6 million people contracted TB globally in 2022 [1]. In 2022, the Presumptive TB Examination Rate (PTBER) for the country increased to 1281 per lakh population, marking a 68% rise from 763 in 2021 [2]. TB is caused by *Mycobacterium tuberculosis*. The emergence of drug-resistant strains poses a significant global threat, leading to the development of Multiple Drug-Resistant Tuberculosis (MDR-TB), Extreme Drug-Resistant Tuberculosis (XDR-TB), and Total Drug-Resistant Tuberculosis (TDR-TB). Till now, several targets have been explored for anti-tubercular activity. Fatty acid synthesis is particularly attractive for the rational design of novel therapeutic [3].

Fatty acids constitute the primary metabolites produced by a complex and indispensable biosynthetic pathway. Microbial fatty acid synthesis is a tightly regulated process involving multiple enzymatic steps and intricate molecular mechanisms [4, 5].

Fatty acid synthesis is facilitated by fatty acid synthase enzymes, namely FAS-I and FAS-II. Unlike mammals, where FAS-I handles synthesis, *Mycobacterium* employs both FAS-I and FAS-II. This distinction makes FAS-II an appealing focus for anti-tubercular research [6].

Isoxyl (ISO) and Thiacetazone (TAC) are prodrugs historically employed in clinical tuberculosis treatment. Recent findings reveal their efficacy against *Mycobacterium tuberculosis* by targeting the dehydration step in the type II fatty acid synthase pathway [7].

Various chemical groups have been extensively investigated, synthesized, and assessed worldwide for their efficacy against *M. tuberculosis*, demonstrating potential antitubercular activity [8, 9].

Heterocyclic molecules like isoniazid, pyrazinamide, cycloserine, ethionamide, and rifampin emerged as the most widely recognized anti-TB drugs in 1960s. However, the treatment regimen for tuberculosis has remained largely unchanged since then and is associated with significant toxic side effects and the development of drug resistance. FDA approval of bedaquiline in 2012 and delamanid in 2014 followed by the recent FDA approval of pretomanid have proven to be a milestone in antitubercular drug discovery [10].

QSAR stands for Quantitative Structure-Activity Relationship. Here, the biological activity of chemical compounds can be predicted or assessed based on their chemical structure.

AutoQSAR applications vary in terms of the descriptors they automatically compute and the methods they employ, such as decision trees, PLS, and random forests, for generating models [11-13]. CoMFA and CoMSIA are widely recognized as effective and reliable approaches in ligand-based drug discovery systems [14].

Here, we have worked with a set of 50 oxadiazole derivatives to evaluate their antituberculosis activity using both 2D and 3D QSAR techniques. The pMIC<sub>50</sub> values were calculated using Density Functional Theory (DFT) methods. This was done to identify common structural features that contribute to the observed antitubercular activity, which can then be used to predict the activity of new molecules, which will further help in understanding drug design and molecular activity. Here, for 2D-QSAR, Auto-QSAR was performed on those 50 molecules of oxadiazole derivative. For 3D-QSAR, both Atom-based QSAR and Field-based QSAR was performed to understand possible functional groups or features required in a molecule to potentiate the antitubercular activity.

### MATERIALS AND METHODS

All the computer-based experiments conducted for this study were performed using the Schrodinger Maestro software version 11.8.

## Dataset

For this study's purpose, 50 oxadiazole derivatives have been taken from the available literature [15]. The structural variability and its correlation with a broad spectrum of biological activities provided an optimal data set for constructing appropriate QSAR models to forecast activity. The IC<sub>50</sub> values were re-generated into PIC<sub>50</sub> values. The software used for this study was MAESTRO interface [16].

When selecting data for 3D QSAR modelling, several key criteria are to be considered for ensuring the flexibility of the model [17]. Some of the factors include quality of data, diversity of compounds, appropriateness of property, data size, availability and accessibility of dataset. Among the set of molecules, 55% of the data were assigned to the training set, whereas the test set included 45% of the data.

## Alignment of molecules

Using Ligprep module in MAESTRO, Schrodinger the energy of the molecules was reduced. The molecules were then aligned. The tool Flexible ligand alignment was employed in the molecular alignment process, from which Common scaffold alignment was chosen and entries were selected and aligned [18].

In the context of CoMFA and CoMSIA, the Powell method is employed to optimize the alignment of molecular structures and to calculate the field or similarity descriptors. CoMFA and CoMSIA are both methods in 3D QSAR studies to establish correlation between the biological activity of a set of molecules with their 3-dimensional structures and properties [19].

## Preference of training set and test set

Compounds are chosen from both the training and test sets in a manner that the training set comprises every character within the dataset. This is one of the crucial steps to construct a QSAR model [20].

## Model development

Phase Module was used for building 3D-Atom-based QSAR model. The internal test set validation was employed to validate these models (Leave One Out), ensuring their reliability [21].

## CoMFA

It is a method that is widely used for drug designing. It depicts the non-bonding interaction of the ligand and the receptor. CoMFA

includes certain prime characters like steric and electrostatic forces. The Partial Least Square (PLS) was employed to determine linear correlation between CoMFA and CoMSIA. 5 factors were initially set [22].

R<sup>2</sup> and Q<sup>2</sup> are the statistical metrics used to evaluate the quality of the 3D-QSAR (three-dimensional QSAR models generated. R<sup>2</sup> ranges from 0 to 1, where 1 is the perfect fit, indicating that the model describes all the variability. The Q<sup>2</sup> determines the accurately predicts the activity of the new compounds. Q<sup>2</sup> ranges from negative to 1, where the values closer to 1 demonstrates better predictive ability.

Even though CoMFA provides multiple advantages, it still has few limitations that is why CoMSIA is regarded to be better than CoMFA.

## CoMSIA

Comparative Molecular Similarity Indices Analysis correlates the biological activity with the compound's structural properties. In the first step of CoMSIA i. e., the field generation molecular properties of the fields like steric, electrostatic, hydrophobic, and hydrogen-bond donor/acceptor fields were calculated. And in later steps, alignment, grid construction and analysis were conducted. CoMSIA offers better and flexible grid generation. The PLS factor was set to 5 here [23].

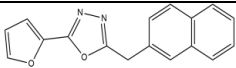
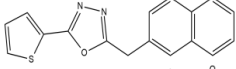
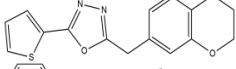
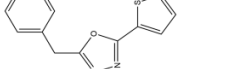
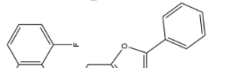

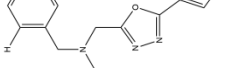
## Validation parameters

In 3D QSAR, R<sup>2</sup> is a value that provides information on how well the model fits the training set. Q<sup>2</sup> is necessary of predictive measures and for the development of a robust model. Higher Q<sup>2</sup> values yield a better predictive value. Leave one out cross-validation is one of the techniques that has been used in this study.

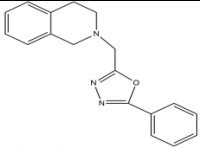
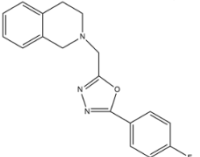
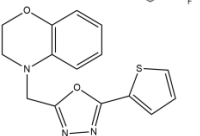
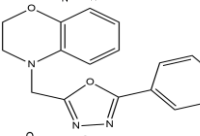
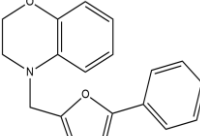
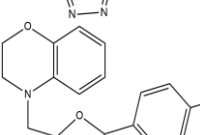
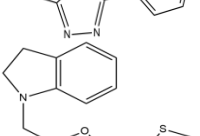
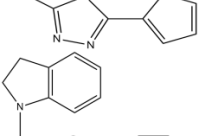
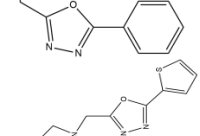
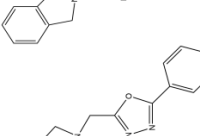
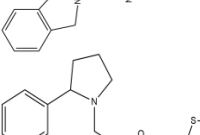
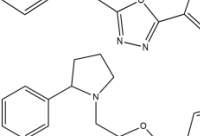
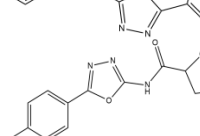
## AUTO QSAR

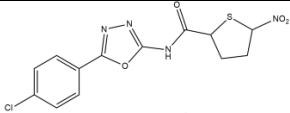
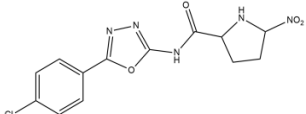
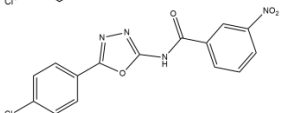
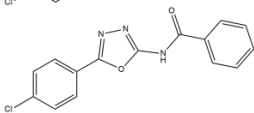
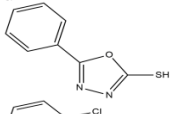
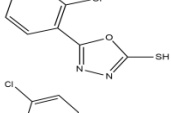
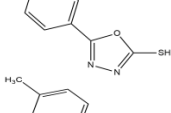
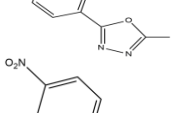
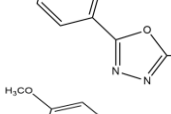
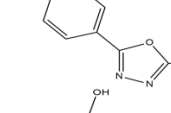
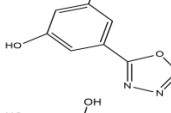
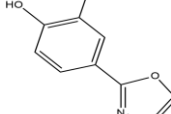
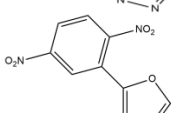
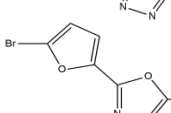
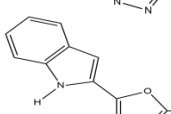
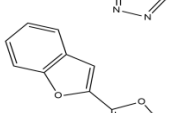
Auto QSAR is the compilation workflow of several processes, such as descriptor generation, feature selection and model training. For this study, Kernel-based Partial Least Squares (KPLS) was used as it extends the capability of the PLS. The QSAR model generation involves a few steps. The process begins with the selection of the datasets that include chemical structures and their corresponding biological activity. The descriptors were generated by importing the structures and topological descriptors were calculated and computed [24]. Following to which feature selection was made and computation was done. Finally, the models were validated using the datasets.

**Table 1: Molecules with structures for QSAR research, along with datasets, projected activities, and measured biological activities**

Compound no.	Structures	MIC	PIC <sub>50</sub> Value	Datasets
1.		1.1	9	Training
2.		5.7	8.244125	Training
3.		0.8	9.09691	Training
4.		1.1	8.958607	Test
6.		0.4	9.39794	Training
7.		0.5	9.30103	Test
8.		0.6	9.221849	Test

Compound no.	Structures	MIC	PIC <sub>50</sub> Value	Datasets
9.		0.6	9.221849	Training
10.		0.9	9.045757	Training
11.		6.8	8.167491	Training
12.		10.8	7.966576	Training
13.		0.7	9.154902	Training
14.		5.5	8.259637	Training
15.		6	8.221849	Training
16.		4	8.39794	Training
17.		0.8	9.09691	Test
18.		1.7	8.769551	Training
19.		0.2	9.69897	Test
20.		0.7	9.154902	Training
21.		3.7	8.431798	Training

Compound no.	Structures	MIC	PIC <sub>50</sub> Value	Datasets
22.		7.7	8.113509	Training
23.		4.7	8.327902	Test
24.		1.8	8.744727	Training
25.		2.8	8.552842	Test
26.		1.8	8.744727	Training
27.		8.3	8.080922	Training
28.		2.1	8.677781	Training
29.		2.3	8.638272	Training
30.		6.7	8.173925	Test
31.		7.5	8.124939	Training
32.		9.9	8.004365	Training
33.		8.3	8.080922	Test
34.		23	7.638272	Training

Compound no.	Structures	MIC	PIC <sub>50</sub> Value	Datasets
35.		44	7.356547	Training
36.		31.25	7.50515	Training
37.		93	7.031517	Test
38.		52	7.283997	Training
39.		12.3	7.910095	Test
40.		100	7	Training
41.		25	7.60206	Training
42.		49.9	7.301899	Test
43.		13.8	7.860121	Training
44.		99.9	7.000435	Training
45.		99.9	7.000435	Training
46.		49.9	7.301899	Training
47.		24.6	7.609065	Training
48.		6	8.221849	Training
49.		5.98	8.221849	Test
50.		5.96	8.224754	Test

## RESULTS AND DISCUSSION

## Atom-based 3D QSAR analysis

An ideal data set for building suitable QSAR models to forecast activity was offered by the structural variability and its association with a wide range of biological activities. A dataset of 50 molecules

was used to create this model. The training set's 83% split was then maintained with PLS factor set to five. The scattered plot's best-fit line was obtained. A better model with highest activity was selected out of 5 different molecules. The selected model had  $R^2$  of (0.979) and  $Q^2$  of (0.9558). Table 2 displays the atom-based QSAR data for the chosen model with five PLS factors.

Table 2: Statistics of atom-based QSAR with five best PLS factors

Factors	SD	$R^2$	$r^2_{cv}$	$r^2$ Scramble	Stability	F	P	RMSE	$Q^2$	Pearson-R
1	0.4992	0.5114	0.4305	0.2395	0.992	84.8	3.09e-14	0.54	0.4518	0.7037
2	0.2753	0.8532	0.636	0.3601	0.882	232.6	4.61e-34	0.36	0.7536	0.8777
3	0.1756	0.941	0.8046	0.4434	0.914	420	1.95e-48	0.25	0.8858	0.9448
4	0.1355	0.9653	0.8362	0.4875	0.908	542.7	4.49e-56	0.19	0.9295	0.967
5	0.1063	0.979	0.8721	0.505	0.907	716.4	5.05e-63	0.15	0.9558	0.9797

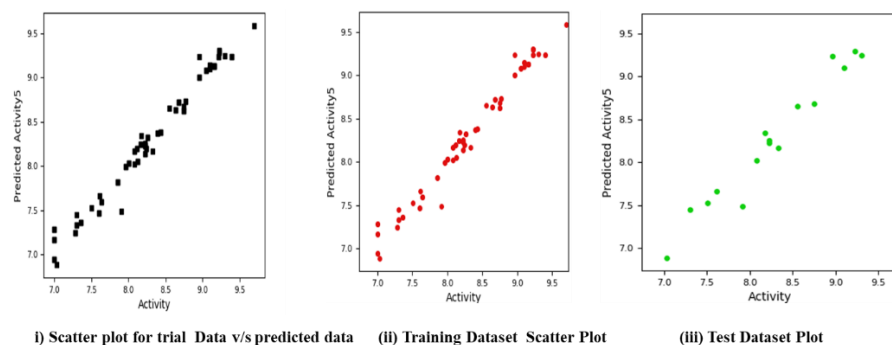


Fig. 1: Atom-based 3D QSAR scatter plot illustrating the relationship between observed and expected activity

Each point in the plot represents a molecule, with its position indicating how well the predicted activity matches the observed activity. The data

points are lying close to the diagonal line ( $y = x$ ), indicating a good predictive model where predicted and observed activities are similar.

Table 3: Results from the QSAR analysis of pharmacophoric features

Factors	H-bond donor	Hydrophobic interaction	Negative ionic	Positive ionic	Electron withdrawing
1	0.039151	0.629508	0.003606	0.004007	0.223044
2	0.041603	0.630768	0.000560	0.000622	0.233347
3	0.042138	0.614565	0.003819	0.004243	0.253473
4	0.041169	0.613056	0.005986	0.006651	0.256295
5	0.041491	0.603524	0.007941	0.008823	0.264063

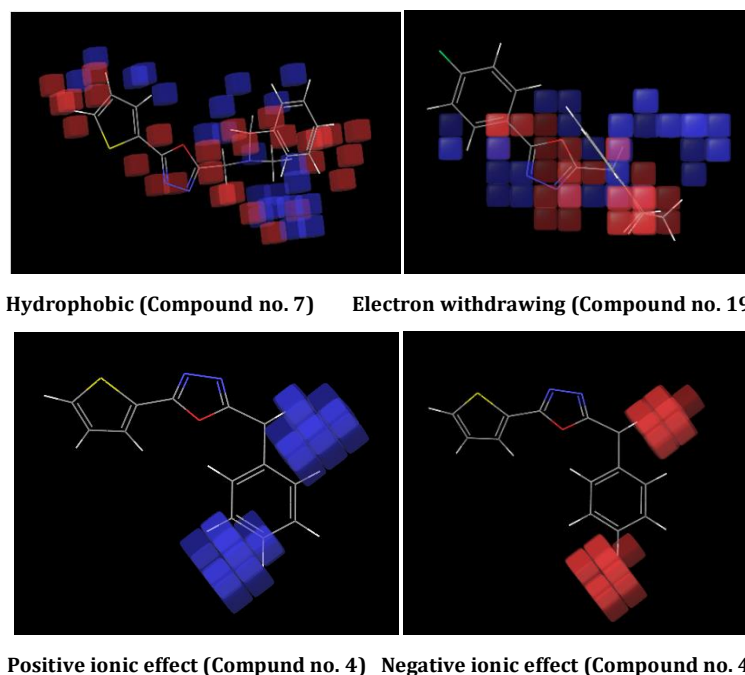


Fig. 2: Hydrophobic/non-polar visualization

### 3D QSAR interpretation

Table 3 illustrates the 3D QSAR analysis across electron-withdrawing, negative, and positive ionic interactions in addition to hydrophobic interactions. According to established activity criteria, dark blue areas indicate positive activity while red portions indicate negative activity. The QSAR model's visual aids facilitate comprehension of the correlation between the biological efficacy and structural features of the ligand molecule as well as the effects of functional group substitution on activity [25, 26].

#### Interpretation of atom-based 3D QSAR

In fig. 2. Hydrophobic (Compound no. 7), the visualization highlights the hydrophobic regions of Compound 7, indicating areas where non-polar interactions may play a significant role in its biological activity. Electron Withdrawing (Compound no. 19), visualization shows the electron-withdrawing regions of Compound 19, illustrating areas where these properties may influence the compound's biological activity.

Positive Ionic Effect (Compound no. 4) visualization highlights regions of Compound 4 areas where positively charged interactions could significantly impact the compound's biological activity. Negative Ionic Effect (Compound no. 4), illustrates regions indicating

areas where negatively charged interactions might influence its biological activity.

#### Visualisation and analysis of 2D QSAR

Molecular structures and the activity patterns that correspond with them are comprehensively visualized using the 2D canvas in 2D QSAR that is linked with kernel-based Partial Least Squares (PLS). Effective model interpretation and prediction are made easier by this intuitive approach, which aids in identifying the relationships between molecular descriptors and biological activities [27, 28].

The best model for correctly predicting activity was the third one, which showed good results on both the training and test datasets. Using five KPLS factors, the test set had an RMSE of 0.3733 and a Q-squared value of 0.7163, whereas the training set had an R-squared value of 0.7817 and a standard deviation of 0.3433. Table 4 provides the statistical features of the 2D QSAR model based on fingerprints. The 2D QSAR fingerprint depiction of the linear model is shown in fig. 4, with red and blue regions denoting, respectively, positive and negative activity effects. The scatter plot for both the training and test datasets is provided. This plot illustrates the relationship between the predicted and actual biological activities, allowing for the assessment of the model's accuracy and predictive performance.

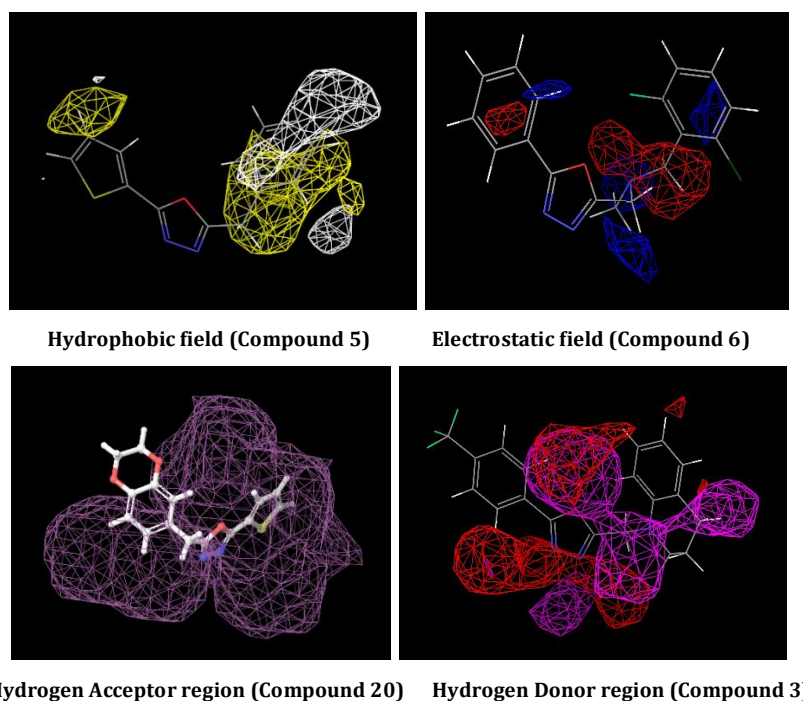


Fig. 3: Representation of 3D Field based QSAR

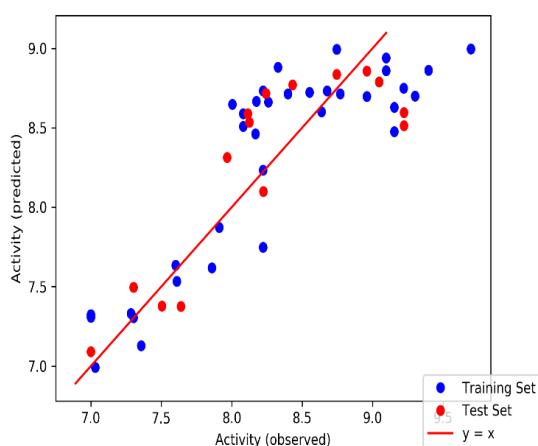


Fig. 4: Scatter plot for both training and test dataset

Table 4: Observations of the models

KPLS factors	Training		Test	
	SD	R <sup>2</sup>	RMSE	Q <sup>2</sup>
1	0.3918	0.7328	0.3626	0.7103
2	0.3996	0.7219	0.3672	0.7029
3	0.3433	0.7817	0.3733	0.7163
4	0.3596	0.7678	0.3790	0.6835
5	0.3760	0.7615	0.3870	0.6700

The 2D and 3D QSAR activity results provide valuable insights for evaluating antitubercular activity by allowing the prediction of how structural variations in oxadiazole derivatives influence their effectiveness against TB. As evident, incorporation of Electron withdrawing group and hydrophobic group was found to be beneficial in enhancing the antitubercular activity of the oxadiazole derivatives. The high predictive accuracy of the models, as evidenced by Q<sup>2</sup> and R<sup>2</sup> values, underscores their reliability in guiding the design of new compounds with enhanced antitubercular properties.

### CONCLUSION

The 3D QSAR model and 2D QSAR model were designed, and suitable models were generated, which were found to be useful for predicting the oxadiazole derivatives for the anti-TB activity. The given study underscores the credibility of derived QSAR model. A high relationship between experimental and predicted activity values was observed, which shows oxadiazole with many options for structural alterations to create possible compounds with strong anti-TB activity and to forecast the activity of any unidentified derivative. The data reported by the QSAR models offers essential guidance for the design of new oxadiazole molecules targeting Tuberculosis.

### ACKNOWLEDGEMENT

The authors are thankful to Manipal College of Pharmaceutical Sciences for providing the facilities to carry out this work.

### FUNDING

Nil

### AUTHORS CONTRIBUTIONS

Neha H. Suvarna was involved in writing the manuscript, conducting the literature search, performing research work, and interpreting the results. Vikshith Raj and Shihabudheen Harees contributed to writing the manuscript and conducting research work. Jessy Elizabeth Mathew provided supervision, critical review, and literature search. Lalit Kumar was involved in supervision, critical review, and literature search. Ruchi Verma contributed by providing the idea, designing the study, supervising, performing critical reviews, writing and editing the manuscript, conducting the literature search, and involved in research work.

### CONFLICT OF INTERESTS

The authors declare no conflict of interest

### REFERENCES

- Global tuberculosis report 2023. Geneva: World Health Organization. License: CC BY-NC-SA 3.0 IGO; 2023. Available from: <https://www.who.int/teams/global-tuberculosis-programme/tb-reports/global-tuberculosis-report-2023>.
- Central TB. Division Ministry of Health and Family Welfare, 3, Sansad Marg, Janpath, New Delhi. Available from: <http://www.tbcindia.gov>.
- Seung KJ, Keshavjee S, Rich ML. Multidrug-resistant tuberculosis and extensively drug-resistant tuberculosis. Cold Spring Harb Perspect Med. 2015;5(9):a017863. doi: [10.1101/cshperspect.a017863](https://doi.org/10.1101/cshperspect.a017863), PMID [25918181](https://pubmed.ncbi.nlm.nih.gov/25918181/).
- Beld J, Lee DJ, Burkart MD. Fatty acid biosynthesis revisited: structure elucidation and metabolic engineering. Mol Biosyst. 2015 Jan;11(1):38-59. doi: [10.1039/c4mb00443d](https://doi.org/10.1039/c4mb00443d), PMID [25360565](https://pubmed.ncbi.nlm.nih.gov/25360565/).
- Odhar HA, Hashim AF, Ahjel SW, Humadi SS. Virtual screening of FDA-approved drugs by molecular docking and dynamics simulation to recognize potential inhibitors against mycobacterium tuberculosis enoyl acyl carrier protein reductase enzyme. Int J App Pharm. 2024;16(1):261-6. doi: [10.22159/ijap.2024v16i1.49471](https://doi.org/10.22159/ijap.2024v16i1.49471).
- Asgaonkar KD, Mote GD, Chitre TS. QSAR and molecular docking studies of oxadiazole ligated pyrrole derivatives as enoyl ACP (CoA) reductase inhibitors. Sci Pharm. 2014;82(1):71-85. doi: [10.3797/scipharm.1310-05](https://doi.org/10.3797/scipharm.1310-05), PMID [24634843](https://pubmed.ncbi.nlm.nih.gov/24634843/), PMCID [PMC3951234](https://pubmed.ncbi.nlm.nih.gov/PMC3951234/).
- Grzegorzewicz AE, Eynard N, Quemard A, North EJ, Margolis A, Lindenberger JJ. Covalent modification of the mycobacterium tuberculosis FAS-II dehydratase by Isoxyl and thiacetazone. ACS Infect Dis. 2015 Feb 13;11(2):91-7. doi: [10.1021/id500032q](https://doi.org/10.1021/id500032q), PMID [25897434](https://pubmed.ncbi.nlm.nih.gov/25897434/).
- Sharma S, Sharma PK, Kumar N, Dudhe R. A review on various heterocyclic moieties and their antitubercular activity. Biomed Pharmacother. 2011 Jul;65(4):244-51. doi: [10.1016/j.biopha.2011.04.005](https://doi.org/10.1016/j.biopha.2011.04.005), PMID [21715130](https://pubmed.ncbi.nlm.nih.gov/21715130/).
- Thomas A, BV, KU SS, MVV. Development of novel 1, 3, 4-thiadiazoles as antitubercular agents synthesis and *in vitro* screening. Int J Curr Pharm Sci. 2023;15(3):37-41. doi: [10.22159/ijcpr.2023v15i3.3009](https://doi.org/10.22159/ijcpr.2023v15i3.3009).
- Dasmahapatra U, Chanda K. Synthetic approaches to potent heterocyclic inhibitors of tuberculosis: a decade review. Front Pharmacol. 2022;13:1021216. doi: [10.3389/fphar.2022.1021216](https://doi.org/10.3389/fphar.2022.1021216), PMID [36386156](https://pubmed.ncbi.nlm.nih.gov/36386156/).
- Bastikar V, Bastikar A, Gupta P. Quantitative structure-activity relationship-based computational approaches. Computational Approaches for Novel Therapeutic and Diagnostic Designing to Mitigate Sars-Cov-2 Infection; 2022. p. 191-205. doi: [10.1016/B978-0-323-91172-6.00001-7](https://doi.org/10.1016/B978-0-323-91172-6.00001-7).
- De Oliveira MT, Katekawa E. On the virtues of automated quantitative structure-activity relationship: the new kid on the block. Future Med Chem. 2018;10(3):335-42. doi: [10.4155/fmc-2017-0170](https://doi.org/10.4155/fmc-2017-0170), PMID [29393678](https://pubmed.ncbi.nlm.nih.gov/29393678/).
- Suhane S, Nerkar AG, Modi K, Sawant SD. 2D and 3D-qsar analysis of amino (3-((3, 5-difluoro-4-methyl-6-phenoxypyridine-2-yl) oxy) phenyl) methaniminium derivatives as factor xa inhibitor. Int J Pharm Pharm Sci. 2019;11(2):104-14. doi: [10.22159/ijpps.2019v11i2.21067](https://doi.org/10.22159/ijpps.2019v11i2.21067).
- Ray R, Shenoy GG, Kumar TN. A comparative study of 1D descriptors supported CoMFA and CoMSIA QSAR models to gain novel insights into 1,2,4-triazoles acting as antitubercular agents. Curr Comput Aided Drug Des. 2021;17(2):281-93. doi: [10.2174/1573409916666200302115432](https://doi.org/10.2174/1573409916666200302115432), PMID [32116196](https://pubmed.ncbi.nlm.nih.gov/32116196/).
- Hosseini S, Ketabi S, Hasheminasab G. QSAR study of antituberculosis activity of oxadiazole derivatives using DFT calculations. J Recept Signal Transduct Res. 2022 Oct;42(5):503-11. doi: [10.1080/10799893.2022.2044860](https://doi.org/10.1080/10799893.2022.2044860), PMID [35263550](https://pubmed.ncbi.nlm.nih.gov/35263550/).
- Ireoluwa YJ, Temidayo OA, Olukayode OB, Mohammed AI, Tamonokorite AS, Onyedika G ANI, Elijah OO, Friday MD, Olusola MA, Bankole EO, Funmilola OA. Insights into features and lead optimization of novel type 1/2 inhibitors of p38α mitogen-activated protein kinase using QSAR, quantum mechanics, bioisostere replacement and ADMET studies. Results Chem. 2020;2:100044. doi: [10.1016/j.rechem.2020.100044](https://doi.org/10.1016/j.rechem.2020.100044).
- Cherkasov A, Muratov EN, Fourches D, Varnek A, Baskin II, Cronin M. QSAR modeling: where have you been where are you going to. J Med Chem. 2014;57(12):4977-5010. doi: [10.1021/jm4004285](https://doi.org/10.1021/jm4004285), PMID [24351051](https://pubmed.ncbi.nlm.nih.gov/24351051/), PMCID [PMC4074254](https://pubmed.ncbi.nlm.nih.gov/PMC4074254/).
- Ali A, Abdellattif MH, Ali A, AbuAli O, Shahbaaz M, Ahsan MJ. Computational approaches for the design of novel anticancer compounds based on pyrazolo[3,4-d]pyrimidine derivatives as



- TRAP1 inhibitor. *Molecules*. 2021;26(19):5932. doi: [10.3390/molecules26195932](https://doi.org/10.3390/molecules26195932), PMID [34641473](https://pubmed.ncbi.nlm.nih.gov/34641473/).
19. Lorca M, Morales Verdejo C, Vasquez Velasquez D, Andrades Lagos J, Campanini Salinas J, Soto Delgado J. Structure activity relationships based on 3D-QSAR CoMFA/CoMSIA and design of aryloxypropanol amine agonists with selectivity for the human  $\beta$ 3-adrenergic receptor and anti-obesity and anti-diabetic profiles. *Molecules*. 2018 May 16;23(5):1191. doi: [10.3390/molecules23051191](https://doi.org/10.3390/molecules23051191), PMID [29772697](https://pubmed.ncbi.nlm.nih.gov/29772697/).
  20. Vilar S, Costanzi S. Predicting the biological activities through QSAR analysis and docking-based scoring. *Methods Mol Biol*. 2012;914:271-84. doi: [10.1007/978-1-62703-023-616](https://doi.org/10.1007/978-1-62703-023-616), PMID [22976034](https://pubmed.ncbi.nlm.nih.gov/22976034/).
  21. Ashraf N, Asari A, Yousaf N, Ahmad M, Ahmed M, Faisal A. Combined 3D-QSAR molecular docking and dynamics simulations studies to model and design TTK inhibitors. *Front Chem*. 2022;10:1003816. doi: [10.3389/fchem.2022.1003816](https://doi.org/10.3389/fchem.2022.1003816), PMID [36405310](https://pubmed.ncbi.nlm.nih.gov/36405310/), PMCID [PMC9666879](https://pubmed.ncbi.nlm.nih.gov/PMC9666879/).
  22. Kim JH, Jeong JH. Structure-activity relationship studies based on 3D-QSAR CoMFA/CoMSIA for thieno-pyrimidine derivatives as triple-negative breast cancer inhibitors. *Molecules*. 2022;27(22):7974. doi: [10.3390/molecules27227974](https://doi.org/10.3390/molecules27227974), PMID [36432075](https://pubmed.ncbi.nlm.nih.gov/36432075/), PMCID [PMC9698756](https://pubmed.ncbi.nlm.nih.gov/PMC9698756/).
  23. Srivastava V, Kumar A, Mishra BN, Siddiqi MI. CoMFA and CoMSIA 3D-QSAR analysis of DMMP derivatives as anti-cancer agents. *Bioinformation*. 2008 Jun 27;2(9):384-91. doi: [10.6026/97320630002384](https://doi.org/10.6026/97320630002384), PMID [18795111](https://pubmed.ncbi.nlm.nih.gov/18795111/).
  24. Dong J, Cao DS, Miao HY, Liu S, Deng BC, Yun YH. ChemDes: an integrated web-based platform for molecular descriptor and fingerprint computation. *J Cheminform*. 2015;7:60. doi: [10.1186/s13321-015-0109-z](https://doi.org/10.1186/s13321-015-0109-z), PMID [26664458](https://pubmed.ncbi.nlm.nih.gov/26664458/).
  25. Ahmed M, Ganesan A, Barakat K. Leveraging structural and 2D-QSAR to investigate the role of functional group substitutions conserved surface residues and desolvation in triggering the small molecule induced dimerization of hPD-L1. *BMC Chem*. 2022;16(1):49. doi: [10.1186/s13065-022-00842-w](https://doi.org/10.1186/s13065-022-00842-w), PMID [35761353](https://pubmed.ncbi.nlm.nih.gov/35761353/).
  26. Samridhi Thakral, Vikramjeet Singh. Biological evaluation, QSAR and molecular modeling studies of 2,4-dichlorobenzoic acid derivatives as antimicrobial agents. *Asian J Pharm Clin Res*. 2019;12(4):98-105. doi: [10.22159/ajpcr.2019.v12i4.31631](https://doi.org/10.22159/ajpcr.2019.v12i4.31631).
  27. Patel RT, Pasha TY, Patel S. 2D-QSAR study on some novel dihydropyrimidine-4-carbonitrile analogs as an antifungal activity. *Int J Pharm Pharm Sci*. 2023;15(3):29-34. doi: [10.22159/ijpps.2023v15i3.47008](https://doi.org/10.22159/ijpps.2023v15i3.47008).
  28. Martinez Mayorga K, Rosas Jimenez JG, Gonzalez Ponce K, Lopez Lopez E, Neme A, Medina Franco JL. The pursuit of accurate predictive models of the bioactivity of small molecules. *Chem Sci*. 2024;15(6):1938-52. doi: [10.1039/d3sc05534e](https://doi.org/10.1039/d3sc05534e), PMID [38332817](https://pubmed.ncbi.nlm.nih.gov/38332817/).